

# Engagement of CD99 Induces Apoptosis Through a Calcineurin-Independent Pathway in Ewing's Sarcoma Cells

Hae Won Sohn,\* Eun Young Choi,\*†  
Soon Ha Kim,\* Im-soon Lee,\*† Doo Hyun Chung,\*  
Uhn A Sung,\* Duck Ho Hwang,‡ Sa Sun Cho,‡  
Byung Hoon Jun,§ Ja June Jang,\* Je Geun Chi,\*  
and Seong Hoe Park\*†

From the Departments of Pathology\* and Anatomy,† Seoul National University College of Medicine, and Institute of Allergy and Clinical Immunology,‡ Seoul, and the Department of Otolaryngology,§ Inje University College of Medicine, Kimbae, Korea

**Programmed cell death (PCD) is a prominent feature of the development of the immune and nervous systems. In both systems, widespread PCD occurs in primitive progenitor cells during development. In this study, we demonstrated that Ewing's sarcoma (ES) cells, undifferentiated neural precursors, underwent apoptosis upon engagement of CD99 with anti-CD99 monoclonal antibody. Apoptosis via CD99 occurred only in the undifferentiated state of ES cells, but not in differentiated ES cells. CD99-induced apoptosis in ES cells appeared to require *de novo* synthesis of RNA and protein as well as caspase activation. Cyclosporin A, known to be a potent inhibitor of both calcineurin activation and mitochondrial permeability transition pore opening, inhibited CD99-mediated apoptosis, whereas FK-506, a specific calcineurin inhibitor, did not, indicating the induction of CD99-mediated apoptosis through a calcineurin-independent pathway. Furthermore, the dying cells displayed the reduction of mitochondrial transmembrane potential ( $\Delta\Psi_m$ ). These results suggest that CD99 engagement induce CsA-inhibitable mitochondrial permeability transition pore opening, followed by a reduction of  $\Delta\Psi_m$  and caspase activation, thereby leading to apoptosis. Based on these results, we suggest the possible involvement of CD99 in the apoptotic processes that occur during nervous system development and also its application in immunotherapeutic trials for ES cases. (*Am J Pathol* 1998, 153:1937-1945)**

Apoptosis, or programmed cell death (PCD), is the mechanism by which cells die through the activation of their intrinsic suicide program in response to changes in ex-

ternal milieu or irreparable cell damages. Apoptosis, in which the cell actively participates in its demise, has been characterized by morphological changes such as chromatin condensation, nuclear fragmentation, internucleosomal DNA fragmentation, and cytoplasmic blebbing.<sup>1</sup> Apoptosis requires that the dying cell be metabolically active, and is often dependent on RNA and protein synthesis.<sup>2,3</sup>

Recently, various triggering factors and processes of apoptosis have been widely investigated *in vitro* and *in vivo*.<sup>4,5</sup> One of the common initial manifestations of the apoptotic process, irrespective of cell types and inducing stimuli, is a disruption of mitochondrial membrane function, including a dissipation of the mitochondrial transmembrane potential ( $\Delta\Psi_m$ ) due to the opening of the mitochondrial permeability transition (PT) pores.<sup>4</sup> In many systems, mitochondrial PT pore opening is inhibited by cyclosporin A (CsA)<sup>6-8</sup> via a mechanism involving a mitochondrial cyclophilin, but not by calcineurin.<sup>6</sup> Despite the extensive studies on PCD during development, little is known about the major cell surface proteins controlling PCD and its intracellular signaling pathway at the early stage of neural ontogeny.

Ewing's sarcoma (ES) is a rare, small-round-cell undifferentiated tumor of bone and soft tissues. ES has been described to represent the stage of either very early pluripotential cells or primitive neuroectodermal cells<sup>9,10</sup> that can differentiate along a neuronal, glial, Schwannian, melanocytic, neuroendocrine, or even ectomesenchymal pathway. ES is considered to be closely related to primitive neuroectodermal tumor (PNET), because they share a common chromosomal abnormality and the high expression of CD99 molecules on their cell surfaces. However, they have some differences in neuronal differentiation potential. PNET has neuronal features such as dense core granules, whereas ES lacks any trace of neuronal differentiation.<sup>11,12</sup> Recently, *in vitro* culture studies have described that ES cell lines possess the ability to differentiate along neuronal pathways in response to various

Supported in part by a grant (KOSEF 95-0403-10-01-3) from the Korean Science and Engineering Foundation and a research grant ('95) from the Seoul National University Hospital Research Fund.

Accepted for publication August 22, 1998.

Address reprint requests to Dr. Seong Hoe Park, Department of Pathology, Seoul National University College of Medicine, 28 Yongon-dong Chongno-gu, Seoul 110-799, Korea. E-mail: pshoe@plaza.snu.ac.kr.

stimuli of differentiating agents.<sup>12-14</sup> One report has shown that the mRNA expression patterns of a neural differentiation marker, NF-L, in ES cell lines were different in PNET, but similar in undifferentiated neural tissues.<sup>12</sup>

CD99 is a ubiquitous 32-kd transmembrane protein encoded by the *mic2* gene,<sup>15</sup> in particular, highly expressed in human cortical thymocytes, Ewing's sarcoma/primitive neuroectodermal tumor (ES/PNET) cells, pancreatic islet cells, and Leydig and Sertoli cells.<sup>16,17</sup> Recently, it has been reported that engagement of CD99 induces homotypic cell aggregation,<sup>18,19</sup> up-regulation of T cell receptor and major histocompatibility complex molecules,<sup>20</sup> and apoptosis in immature thymocytes.<sup>21</sup>

In the present study, we demonstrate that CD99-induced apoptosis occurs only in undifferentiated ES cells, not in differentiated ES cells, as it does in immature cortical thymocytes. We suggest that CD99 might trigger apoptosis in a certain developmental stage during neural ontogeny and also that CD99 might be used as a target for immunotherapy of ES patients.

## Materials and Methods

### Antibodies and Reagents

The monoclonal antibody (MAb) DN16 (IgG<sub>1</sub>) used for CD99 activation was produced in our laboratory and described previously.<sup>22</sup> We purchased rabbit anti-mouse immunoglobulin Ab and FITC-conjugated goat anti-mouse immunoglobulin Ab from Sigma Chemical Co. (St. Louis, MO) and mouse anti-NF-H MAb (NCL-NF200) from Novocastra Laboratories (New Castle upon Tyne, UK). N<sub>6</sub>-O<sub>2</sub>-Dibutyryl adenosine-3,5'-cyclic monophosphate (db-cAMP) and 3,3'-dihexyloxycarbocyanine iodide (DiOC<sub>6</sub>(3)) were purchased from Sigma Chemical Co. Calcium ionophore A23187 was from Boehringer Mannheim Biochemicals (Mannheim, Germany). Apoptosis inhibitors, such as actinomycin D (Act D), cycloheximide (CHX), cyclosporin A (CsA), and EGTA, were also from Sigma Chemical Co. FK-506 was kindly provided by Dr. J. K. Shin (Dana-Farber Cancer Institute). Z-VAD-fmk and Z-FA-fmk were obtained from Enzyme System Products (Livermore, CA).

### Cell Culture

RD-ES (human Ewing's sarcoma), SK-N-MC (human PNET), and SK-N-SH (human neuroblastoma) cells were obtained from the American Type Culture Collection (Rockville, MD), and CADO-ES1 cells (human Ewing's sarcoma) were obtained from the German Collection of Microorganism and Cell Cultures (Braunschweig, Germany). Two human neuroblastoma cell lines, SK-N-AS and SH-SY5Y, were generous gifts of Dr. Chong-Jae Kim (Seoul National University College of Medicine, Seoul, Korea). RD-ES and CADO-ES1 cells were maintained in RPMI 1640 supplemented with 15% and 10% fetal bovine serum (FBS; Life Technology, Gaithersburg, MD), respectively. SK-N-MC, SK-N-SH, SK-N-AS, and SH-SY5Y cells were cultured in Dulbecco's minimal essential me-

dium supplemented with 10% FBS. For differentiation induction of RD-ES and CADO-ES1 cells, the cells were cultured in Dulbecco's minimal essential medium supplemented with 10% FBS in the presence of 2.5 mmol/L and 0.25 mmol/L db-cAMP, respectively. The medium was changed every 3rd day and maintained for up to 12 days.<sup>12</sup>

### Immunofluorescence Staining and Confocal Analysis

For immunofluorescence staining, db-cAMP-treated and untreated ES cells were fixed in 95% methanol for 15 minutes at room temperature, permeabilized with 0.1% Triton X-100 in PBS, and washed three times with PBS containing 1% FBS. The cells were then blocked in 10% FBS for 30 minutes and stained with mouse anti-NF-H MAb overnight at 4°C. After washing three times in PBS containing 1% FBS for 15 minutes, the cells were incubated with fluorescein isothiocyanate (FITC)-conjugated goat anti-mouse immunoglobulin Ab and mounted on the glass with mounting media (GEL/MOUNT, Biomedica Corp., Foster City, CA). Confocal analysis was performed with a 600MRC equipped with an argon/krypton laser (BioRad Labs, Hercules, CA). Green fluorescence was detected at  $\lambda > 515$  nm after excitation at 488 nm.

### Trypan Blue Dye Exclusion Assay

For the MAb-induced cell death assay, cells ( $5 \times 10^5$  cells/well) were placed in 24-well plates and incubated with 10  $\mu$ g/ml anti-CD99 MAb and the secondary Ab for cross-linking of CD99 or the secondary Ab alone for the indicated period. In the inhibition experiment of cell death induced by CD99 or calcium ionophore A23187, RD-ES cells were treated with 10  $\mu$ g/ml anti-CD99 MAb or 10  $\mu$ mol/L A23187, respectively, at 37°C in the presence or absence of 0.1  $\mu$ g/ml Act D, 1.0  $\mu$ g/ml CHX, 0.1 to 200  $\mu$ mol/L CsA, 1.5 mmol/L EGTA containing 1.5 mmol/L MgCl<sub>2</sub>, and various concentrations of FK-506 for the indicated period. To examine the requirement of caspases in CD99-induced apoptosis, RD-ES cells were pretreated with 20  $\mu$ mol/L Z-VAD-fmk (a general caspase inhibitor) or Z-FA-fmk (a control cysteine protease inhibitor) for 2 hours. The cells were then incubated for 6 hours in the presence or absence of DN16 MAb. Cell death was quantified by trypan blue dye exclusion. All experiments were performed at least three times, and a representative result of the experiments is shown in figures.

### Electron Microscopy

Cells were fixed in 2.5% glutaraldehyde in 0.1 mol/L phosphate buffer, pH 7.4, for 24 hours at 4°C. Then they were post-fixed in 0.1% osmium tetroxide in the same solution for 1 hour, dehydrated, transferred to propylene oxide, and embedded in epoxy resin (Polyscience Co., Warrington, PA). Ultrathin sections were stained with saturated aqueous uranyl acetate and lead citrate and ex-

amed under an electron microscope (Hitachi, H-600) at 75 kV.

### Flow Cytometric Analysis

Cells ( $1 \times 10^6$ ) were incubated with anti-CD99 MAb ( $1 \mu\text{g}/100 \mu\text{l}$ ) in PBS containing 1% bovine serum albumin and 0.1% sodium azide for 30 minutes at  $4^\circ\text{C}$ , washed with PBS, and stained with FITC-conjugated goat anti-mouse immunoglobulin Ab. After three washes, cells were analyzed on a FACScan (Becton Dickinson, San Jose, CA).

### TUNEL Labeling

Apoptosis was assessed by TdT-mediated dUTP nick end-labeling (TUNEL) assay<sup>23</sup> using the APO-DIRECT apoptosis detection kit (Pharmingen, San Diego, CA). Control or anti-CD99 Ab-treated cells ( $1 \times 10^6$  to  $2 \times 10^6$ ) were fixed with 4% paraformaldehyde, washed in PBS, resuspended in 70% cold ethanol, and stored overnight. After washing the cells with PBS, the TUNEL assay was performed according to the manufacturer's protocol.

### Assessment of Mitochondrial Transmembrane Potentials

After the induction of apoptosis with anti-CD99 MAb ( $2 \mu\text{g}/\text{ml}$ ) for 2 hours, cells ( $1 \times 10^6$ ) were incubated for 15 minutes in 1 ml of 20 nmol/L DiOC<sub>6</sub>(3) at  $37^\circ\text{C}$ , followed by analysis on a FACScan (excitation, 488 nm; emission, 525 nm).<sup>24</sup> The control experiment was performed in the presence of 50  $\mu\text{mol}/\text{L}$  carbamoyl cyanide *m*-chlorophenylhydrazone (*m*CICCP), an uncoupling agent that abolishes  $\Delta\Psi\text{m}$ , for 15 minutes at  $37^\circ\text{C}$ .

## Results

### Engagement of CD99 Induces Rapid Cell Death Only in Undifferentiated ES Cell Lines

Recently, it has been reported that CD99 mediates apoptosis in immature thymocytes and Jurkat cells.<sup>21</sup> The findings that ES/PNET is a neoplastic counterpart of primitive neuroectodermal cells<sup>9-11</sup> and that these cells express a large amount of CD99 on their surfaces<sup>17,25</sup> led us to ask whether the ligation of CD99 with anti-CD99 MAb DN16 could induce cell death in ES/PNET cell lines. In this experiment, cells from two ES cell lines (RD-ES and CADO-ES1) and one PNET cell line (SK-N-MC) were incubated with DN16 in the presence of cross-linking Ab. Within 2 hours after the DN16 treatment, cell death was clearly observed in the ES cells. Maximal cell death was evident within 6 hours (Figure 1A). However, in SK-N-MC, which has recently turned out to be PNET,<sup>26</sup> CD99-induced cell death did not occur within 6 hours (Figure 1B) or even after 24 hours (data not shown), indicating that CD99 molecules were able to deliver a death signal only in ES cells, but not in SK-N-MC cells. In addition, neuro-

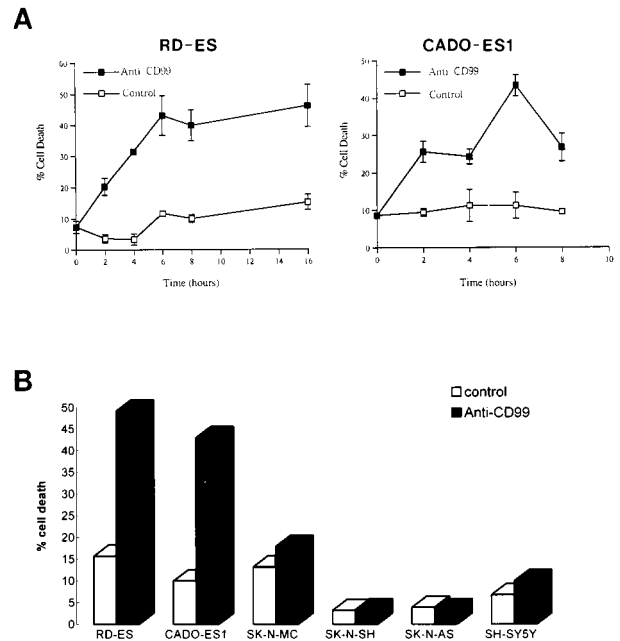


**Figure 1.** Effect of CD99 engagement in ES, PNET, and neuroblastoma cells. **A:** CD99-induced death in RD-ES and CADO-ES1 cells. In 24-well plates,  $5 \times 10^5$  cells/ml of RD-ES and CADO-ES1 cells were plated and incubated with DN16 (anti-CD99 MAb) and the secondary Ab (rabbit anti-mouse immunoglobulin Ab) for cross-linking of CD99 (■) or with the secondary Ab alone (control, □) for the indicated periods of time. All values are means  $\pm$  SD of three separate experiments. **B:** Resistance to CD99-induced cell death in a PNET and three neuroblastoma cell lines. SK-N-MC (PNET cell line) and SK-N-SH, SK-N-AS, and SH-SY5Y (neuroblastoma cell lines) as well as RD-ES and CADO-ES1 (ES cell lines) cells were treated with the secondary Ab alone (control, open bars) or with DN16 (filled bars) for 6 hours as described in A. Percent cell death was assessed by trypan blue dye exclusion and shown as a percentage of dead cells in total cells.

blastoma cells, such as SK-N-SH, SK-N-AS, and SH-SY5Y, were also resistant to CD99-mediated death after a 6-hour engagement (Figure 1B). Among the three types of tumors tested, ie, PNET, neuroblastoma, and ES cells, which differ in their neurogenic potentials and the levels of CD99 expression, ES cells are considered to be the tumor of the most undifferentiated stage.<sup>12,27</sup> As it was necessary to prepare cells in various stages of differentiation, we performed the *in vitro* induction of neural differentiation of RD-ES and CADO-ES1 cells by db-cAMP treatment. After 12 days of the induction of ES cells with db-cAMP, morphological changes such as elongated cytoplasmic process and varicosity formation were observed under phase contrast microscopic examination (Figure 2, B and D). Furthermore, in the indirect immunofluorescence analysis, the expression of NF-H, a neural differentiation marker, was clearly visualized in differentiated CADO-ES1 (Figure 2E) and RD-ES cells (data not shown). As shown in Figure 2E, NF-H was mainly localized in the perinuclear cytoplasm and in the elongated neuritic process of the differentiated CADO-ES1 cells. Subsequent experiments were done on both the undifferentiated and the differentiated ES cells to investigate whether the induction of CD99-mediated apoptosis is dependent on the degree of differentiation. Interestingly, apoptosis occurred only in the undifferentiated form of ES cells (Figure 3A). The expression level of CD99 was

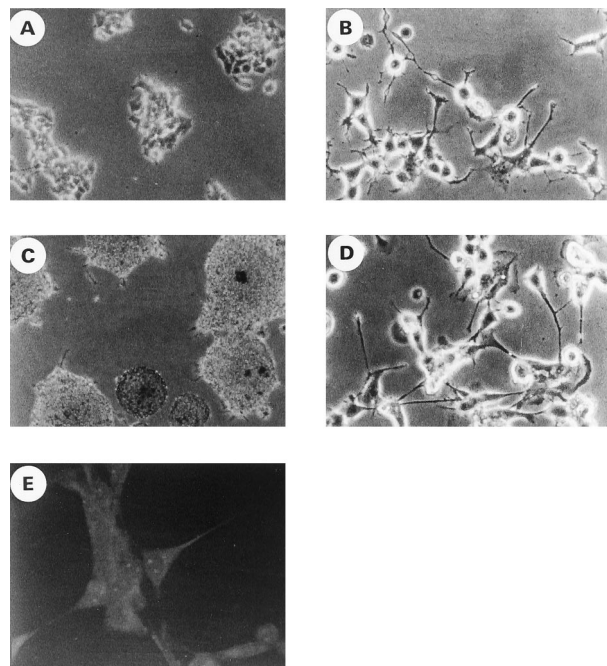


**Figure 2.** The morphological changes and neurofilament expression after the differentiation induction of ES cells with db-cAMP. **A–D:** Cell culture morphology of RD-ES (**A** and **B**) and CADO-ES1 (**C** and **D**) cells under phase contrast microscopy. RD-ES and CADO-ES1 cells were cultured in the absence (**A** and **C**) or presence (**B** and **D**) of db-cAMP for 12 days. The differentiated cells show long cytoplasmic processes, and some neurites terminated in growth cones (**B** and **D**). **E:** Differentiated CADO-ES1 cells were stained with anti-NF-H MAb and analyzed by confocal microscopy. Note the neuritic process and perinuclear localization of NF-H.

dramatically decreased in the differentiated ES cells (Figure 3B). All these data suggest that CD99 can deliver a death signal into undifferentiated ES cells that express CD99 on their surfaces at a high level.

### Engagement of CD99 in RD-ES Cells Induces Typical Ultrastructural Changes Seen in Apoptotic Cells

Apoptosis has been characterized by morphological changes such as chromatin condensation, nuclear fragmentation, internucleosomal DNA fragmentation, and cytoplasmic blebbing.<sup>1</sup> The electron microscopic analysis of RD-ES cells treated with DN16 MAb clearly showed several ultrastructural changes comparable to those of apoptotic cells (Figure 4, A–C), as compared with the control Ab-treated cells (Figure 4D).

CD99-induced apoptosis in RD-ES cells was further confirmed by the TUNEL method.<sup>23</sup> Although a typical ladder pattern of DNA fragmentation was not clear on agarose gel electrophoresis (data not shown), TUNEL assay revealed that the percentage of apoptotic cells in the DN16 MAb-treated RD-ES cells was nearly five times higher than that in the control Ab-treated cells. Approximately 20% of the cells treated with DN16 MAb contained incorporated FITC-dUTP (Figure 5, right), whereas only 4.5% of the control Ab-treated cells were positive for FITC-dUTP (Figure 5, left). It is likely that CD99 induces extremely limited endonuclease activities, as a DNA lad-

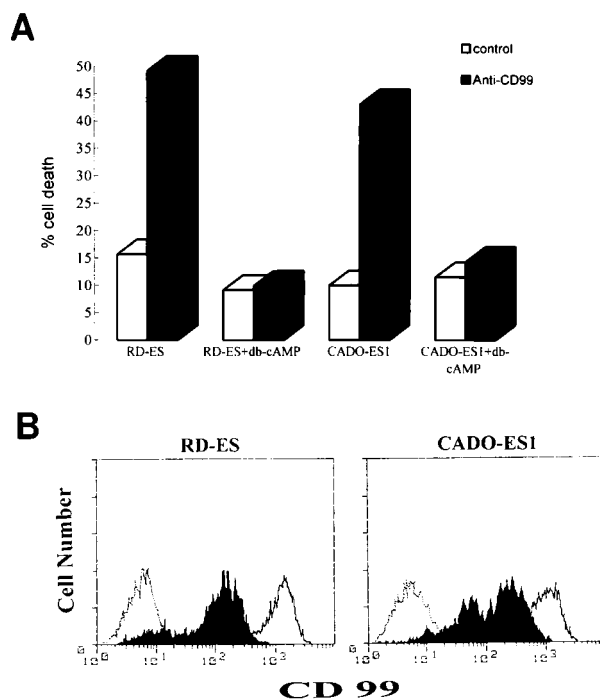


**Figure 3.** Resistance to CD99-induced cell death and the down-regulation of CD99 in the differentiated ES cells. **A:** Resistance to CD99-induced cell death in db-cAMP-treated ES cells. ES cells were cultured in the presence or absence of db-cAMP for 12 days. In 24-well plates, the db-cAMP-treated or untreated cells ( $5 \times 10^5$  cells) were plated and incubated with DN16 (anti-CD99 MAb) and the secondary Ab (rabbit anti-mouse immunoglobulin Ab) for cross-linking of CD99 (filled bars) or with the secondary Ab alone (control, open bars) for 6 hours. All values are the averages of the experiments done in duplicates. The percentage of dead cells was assessed by trypan blue dye exclusion. **B:** Effect of db-cAMP on the expression of CD99. Live cells were gated and analyzed on a FACScan flow cytometer. The expression level of CD99 was markedly reduced in the db-cAMP-treated ES cells (filled areas) as compared with the untreated ES cells (open areas). The dotted line indicates the staining pattern with a negative control Ab.

der pattern was not seen on gel electrophoresis and the labeling intensity of FITC-dUTP was weak.

### De Novo Synthesis Is Necessary for CD99-Mediated Apoptosis in RD-ES Cells

As many apoptotic processes require *de novo* synthesis of RNA and/or protein,<sup>2,3</sup> we tested whether this is also the case in CD99-induced apoptosis in RD-ES cells. As shown in Figure 6, the CD99-mediated apoptosis in RD-ES cells was completely blocked after treatment with a RNA synthesis inhibitor, Act D (Figure 6B), or a protein synthesis inhibitor, CsA (Figure 6C), at the concentration of 0.1  $\mu\text{g/ml}$  or 1.0  $\mu\text{g/ml}$ , respectively. These results indicate that *de novo* synthesis of both RNA(s) and protein(s) are necessary for the process of apoptosis via CD99 in RD-ES cells.

### CD99-Induced Apoptosis in RD-ES Cells Is Blocked by Cyclosporin A but Not by FK-506

An increasing amount of evidence has shown that the alteration of mitochondrial membrane function plays a crucial role in the induction of apoptosis.<sup>28–30</sup> As CsA is

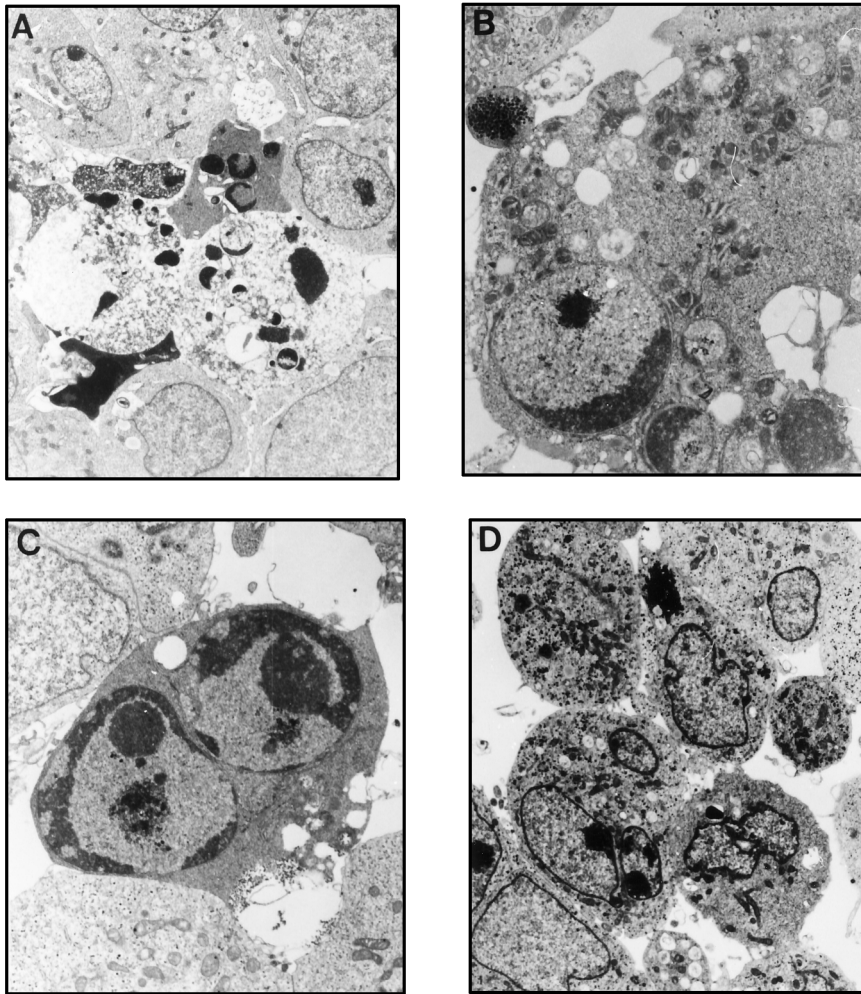


**Figure 4.** Ultrastructural changes in anti-CD99 MAb-treated cells. RD-ES cells were treated with 2  $\mu\text{g/ml}$  DN16 MAb (A–C) or the secondary Ab alone (D) for 6 hours and prepared for electron microscopic examination as described in Materials and Methods. The apoptotic cells displayed karyorrhexis (magnification,  $\times 4500$ ; A) and chromatin condensation with nuclear fragmentation (magnification,  $\times 10,000$ ; C). Some cells show mitochondrial condensation (magnification,  $\times 18,000$ ; B). Cells treated with the secondary Ab alone are shown in D (magnification,  $\times 3500$ ).

a potent inhibitor of mitochondrial PT pore opening,<sup>6,8</sup> we examined the effect of CsA in CD99-induced apoptosis. When RD-ES cells were pretreated with CsA at the various concentrations ranging from 0.1 to 200  $\mu\text{mol/L}$ , CD99-induced apoptosis was completely inhibited at the concentration above 100  $\mu\text{mol/L}$  CsA (Figure 7). It has been well known that CsA can inhibit apoptosis not only through the modification of mitochondrial PT pores but also through inactivation of calcineurin by complex for-

mation with cyclophilin A.<sup>31</sup> Therefore, to rule out the possible involvement of calcineurin in CD99-induced apoptosis, we examined the effect of FK-506, a more selective calcineurin inhibitor, in RD-ES cells. The apoptosis in RD-ES cells was not protected by the treatment of FK-506 (ranging from 10 to 100 nmol/L; Figure 8A), indicating that apoptosis induced by CD99 cannot be blocked by inhibition of calcineurin. Interestingly, calcium ionophore, which induces calcium signaling and activates calcineurin in a calcium-dependent manner, was also able to induce the death of RD-ES cells. Figure 8B shows that both CsA and FK-506 protect RD-ES cells from the calcium-ionophore-induced apoptosis. These data strongly suggest that CD99-induced apoptosis is mediated by mitochondrial PT pore opening, regardless of  $\text{Ca}^{2+}$ /calmodulin-dependent calcineurin activity.

To further investigate the involvement of calcium signaling in CD99 engagement, RD-ES cells were incubated with EGTA, an extracellular  $\text{Ca}^{2+}$ -chelating agent, to prevent the influx of extracellular calcium. Figure 8C showed that removal of extracellular calcium with the combined treatment of 1.5 mmol/L EGTA and 1.5 mmol/L  $\text{MgCl}_2$  did not prevent CD99-induced apoptosis in RD-ES cells, whereas ionophore-induced cell death was inhibited by

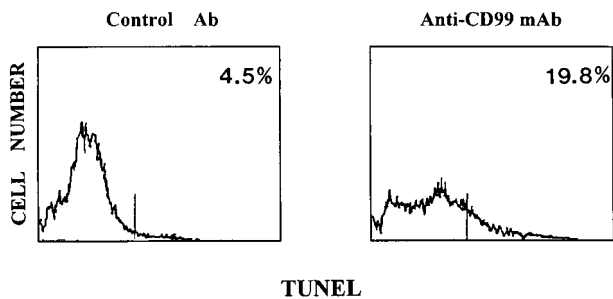
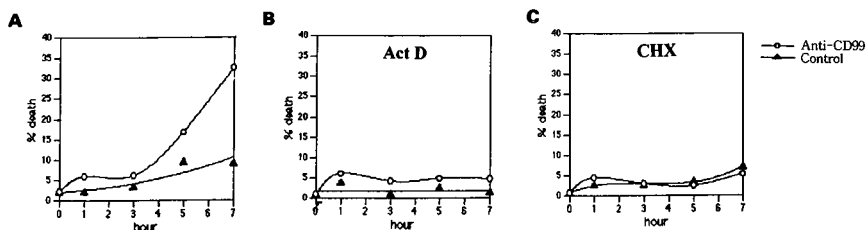


**Figure 5.** Detection of apoptosis by TUNEL method in anti-CD99 MAb-treated RD-ES cells. RD-ES cells were treated with control Ab (left) or DN16 MAb (right), followed by staining for apoptosis by nick end-labeling (TUNEL). The given numbers indicate the percentage of apoptotic TUNEL-positive cells.

**Figure 6.** Requirement of *de novo* synthesis of RNA and protein for CD99-mediated apoptosis in RD-ES cells. In these experiments, RD-ES cells were plated and incubated with anti-CD99 MAb (○) or the secondary Ab alone (▲) in the absence of both (A) or the presence of either 100 ng/ml Act D (B) or 1 μg/ml CHX (C).



EGTA and MgCl<sub>2</sub> pretreatment. These results suggest that CD99-induced cell death may occur through a signal transduction pathway independent of a sustained increase of intracellular calcium.

### Reduction in the $\Delta\Psi_m$ of RD-ES Cells Is Detected after Engagement of Anti-CD99 MAb

To confirm whether CD99-induced cell death in RD-ES is dependent on the reduction of the  $\Delta\Psi_m$ , which is mediated by the opening of mitochondrial PT pores, we used the fluorochrome DiOC<sub>6</sub>(3). As DiOC<sub>6</sub>(3) incorporates into cells in strict nonlinear correlation with  $\Delta\Psi_m$ ,<sup>32</sup> the reduction of  $\Delta\Psi_m$  can be determined by the uptake rate of DiOC<sub>6</sub>(3). Anti-CD99 MAb-treated RD-ES cells exhibited a reduction in the incorporation of DiOC<sub>6</sub>(3), as compared with control Ab-treated cells (Figure 9). With mCICCP, an uncoupling agent of the oxidative phosphorylation that abolishes staining with DiOC<sub>6</sub>(3), we demonstrated that the dye uptake was driven by  $\Delta\Psi_m$  and did not involve significant binding to other cellular components (Figure 9, top). Therefore, we were able to confirm the reduction of the  $\Delta\Psi_m$  in DN16 MAb-treated cells.

### CD99-Induced Apoptosis Is Inhibited by Z-VAD-fmk

Recently, many reports have shown that caspases are crucial for the execution phase of apoptosis.<sup>33,34</sup> To examine whether caspases are required for CD99-induced apoptosis, RD-ES cells were treated with a cell-permeable caspase inhibitor (Z-VAD-fmk) or a control peptide (Z-FA-fmk) for 2 hours before CD99 engagement. As

shown in Figure 10, cell death was almost completely abolished in Z-VAD-pretreated RD-ES cells as compared with that in Z-FA-pretreated or only anti-CD99-treated cells (Figure 10). This result suggests that CD99-induced apoptosis is executed through caspases that are inhibited by Z-VAD-fmk.

### Discussion

In this paper, we report that undifferentiated ES cells are subject to apoptosis upon engagement of CD99 and that the apoptotic process is induced via the reduction of the  $\Delta\Psi_m$  due to mitochondrial PT pore opening.

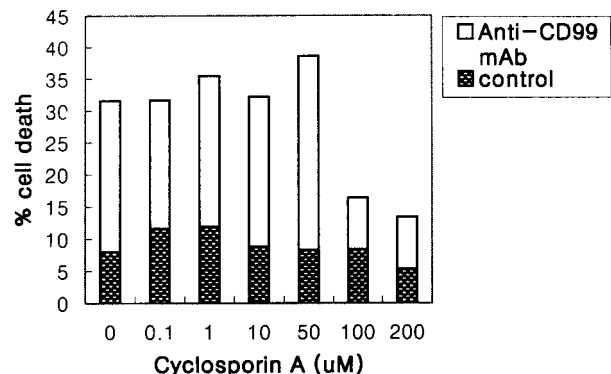


**Figure 7.** Inhibitory effect of CsA on apoptosis induced by anti-CD99 MAb. CsA was preincubated for 1 hour before the induction of apoptosis with anti-CD99 MAb. Results are shown as percentages of dead cells measured by trypan blue dye exclusion.

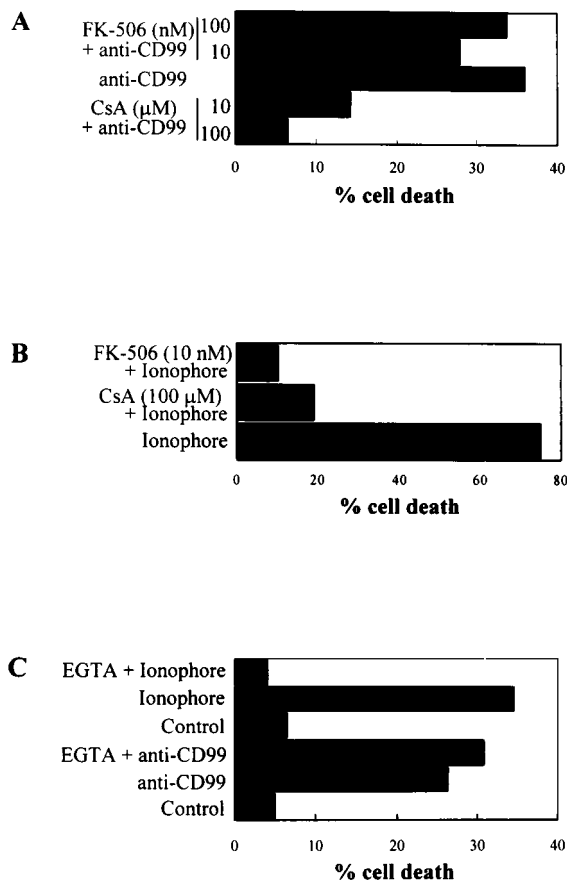


**Figure 8.** Effects of CsA, FK-506, and EGTA on apoptosis induced by anti-CD99 MAb or calcium ionophore. RD-ES cells were preincubated with CsA or FK-506 for 2 hours before the induction of apoptosis by anti-CD99 MAb at 10 μg/ml (A) or calcium ionophore A23187 at 10 μmol/L (B). In the case of EGTA treatment, RD-ES cells were preincubated with a combination of 1.5 mmol/L EGTA and 1.5 mmol/L MgCl<sub>2</sub> for 1 hour before the induction of apoptosis (C). Results are expressed as percentages of dead cells measured by trypan blue dye exclusion.

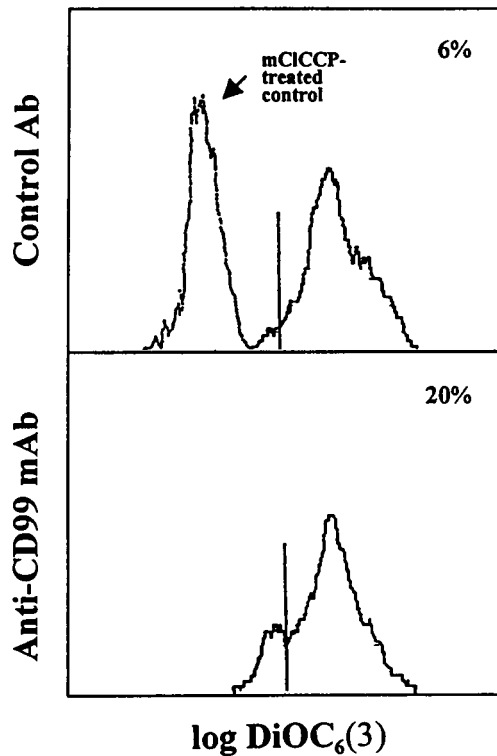


**Figure 9.** Reduction in the  $\Delta\Psi_m$  of RD-ES cells after induction of CD99-mediated apoptosis. RD-ES cells were incubated with control Ab (top) or anti-CD99 MAb (bottom) for 2 hours and stained with DiOC<sub>6</sub>(3). After staining, flow cytometric analysis was performed. Negative control (*mCICCP*-treated cells) is shown in the upper panel. The numbers indicate percentages of DiOC<sub>6</sub>(3)<sup>low</sup> cells among the viable fraction of cells as determined by FSC and SSC. Data are representative of three different experiments.

Recently, it has been reported that CD99-mediated apoptosis occurs in immature thymocytes.<sup>21</sup> CD99-induced cell death in both thymocytes and ES displays many common features, such as typical ultrastructural changes, the inhibition of cell death by caspase inhibitors, the absence of DNA ladder formation, and Fas-independent apoptosis (data not shown). Despite the fact that internucleosomal DNA fragmentation has been shown to be one of the widely accepted hallmarks of the apoptotic cell death, we were not able to observe the

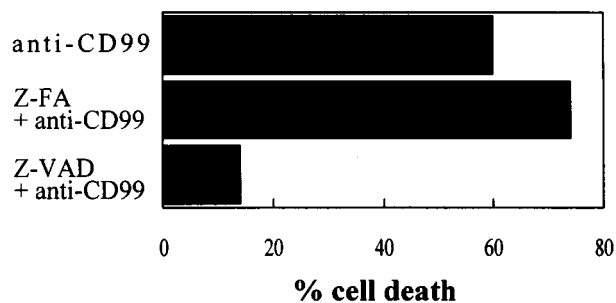


**Figure 10.** Inhibition of CD99-induced apoptosis by a caspase-1, -3, and -9 inhibitor, Z-VAD-fmk. RD-ES cells were pretreated with 20  $\mu\text{mol/L}$  Z-VAD-fmk (a caspase inhibitor) or Z-FA-fmk (a control peptide inhibitor) for 2 hours before CD99 engagement. Apoptosis was induced by 2  $\mu\text{g/ml}$  anti-CD99 MAb for 6 hours and evaluated by trypan blue dye exclusion. Results are expressed as percentages of dead cells. Experiments were performed as duplicates.

obvious DNA fragmentation in this type of apoptosis. Recently, several lines of evidence have shown that caspases, particularly caspase 3, plays an important role in the DNA fragmentation.<sup>33,35</sup> For example, caspase 3 induces the DNA fragmentation by the cleavage of caspase-activated deoxyribonuclease inhibitor (ICAD) or by the inactivation of its CAD-inhibitory effects. ICAD-transformants were resistant to staurosporin-induced DNA degradation, although staurosporin still induced cell death by activating caspases.<sup>35</sup> The findings indicate that the activation of CAD downstream of the caspase cascade is responsible for internucleosomal DNA degradation during apoptosis. The apoptosis through CD99 appeared to be devoid of prominent internucleosomal DNA fragmentation in the two types of cells, thymocytes and ES cells, despite the inhibition by the caspase inhibitors (Figure 10). Therefore, it can be suggested that CD99-induced apoptosis in RD-ES cells might occur through a unique signaling pathway that could induce caspase activation, chromatin condensation, and nucleus fragmentation without the activation of calcium-dependent internucleosomal endonucleases.

Although the CD99-induced apoptosis in both ES cells and thymocytes displays many features in common, these two types of cells show apparent contrast in that ES cells require *de novo* synthesis of RNA and protein (Figure 6), unlike immature thymocytes. It implies that CD99-induced apoptosis in ES cells might function through a metabolically active process that is dependent on RNA and protein synthesis.<sup>2,3</sup>

The pretreatment of CsA protected RD-ES cells from CD99-induced apoptosis. It is well known that the functions of CsA are mediated by the formation of a complex with one of the CsA-binding proteins, cyclophilins, for instance, CsA-cyclophilin D complex for the inhibition of mitochondrial PT pore opening and CsA-cyclophilin A and B complex for the antagonization of calcineurin.<sup>6</sup> It has been recently reported that one of the common manifestations of the apoptotic process is a disruption of mitochondrial membrane functions, including a dissipation of the  $\Delta\Psi_m$  due to the opening of the mitochondrial PT pores.<sup>24</sup> In RD-ES cells, CD99-induced apoptosis was abrogated by CsA pretreatment (Figures 7 and 8A) but not by FK-506 or EGTA (Figure 8, A and C) pretreatment, whereas ionophore-induced apoptosis was inhibited by the pretreatment with the inhibitors (Figure 8, B and C). Furthermore, the engagement of CD99 led to a substantial reduction in the  $\Delta\Psi_m$  (Figure 9). Therefore, the CD99-induced apoptosis in RD-ES cells may occur through the  $\Delta\Psi_m$  disruption due to CsA-inhibitable mitochondrial PT pore opening, which is independent of a sustained increase of intracellular calcium and calcineurin activation. This suggestion is in agreement with the result that the prominent activities of endonucleases, which require intracellular calcium signaling, were virtually absent.

It is very intriguing that engagement of CD99 can trigger apoptosis only in undifferentiated ES cells and not in differentiated ES and PNET cells. The origin of ES has been hypothesized to be derived from a primitive pluripotential cell that can differentiate into cells with neural, Schwannian, melanocytic, neuroendocrine, or even mes-

enchymal features.<sup>9,10</sup> Much evidence has been accumulated for the potential of ES cells to undergo marked neural differentiation *in vitro*.<sup>11-14</sup> One report demonstrates that ES cells express several typical markers of neuronal precursor cells, such as NCAM, LNGFR, and Leu-7. Furthermore, ES cells that are naturally negative for neurofilaments induced the expression of neurofilaments (NF-L, -M, and -H) when cultured in the presence of db-cAMP.<sup>12</sup> These characteristics indicate that ES cells maintain a primitive phenotype and have a potential to differentiate into cells with a neural phenotype. Likewise, ES cells used in our experiment have no evidence of differentiated neuronal features, such as long cytoplasmic processes and the presence of NF-H, a marker of a developing neuron. Upon the treatment of ES cells with db-cAMP, the expression of NF-H became evident (Figure 2). After differentiation, the expression level of CD99 on the cell surfaces was dramatically reduced, and the cells appeared to be resistant to CD99-induced cell death. It is a conceivable explanation that the lack of response to anti-CD99 MAb treatment in the differentiated ES cells might be due to the alteration of an apoptotic signaling pathway via CD99 engagement and/or due to the down-regulation of CD99 expression in the differentiated ES cells. CD99 is also dramatically down-regulated in medullary mature thymocytes in contrast with immature thymocytes. In addition, CD99 engagement induces apoptosis only in immature thymocytes but not in mature thymocytes,<sup>21</sup> suggesting that CD99 induces cell death in a stage-specific manner. We observed similar phenomena in ES cells. This finding suggests that the CD99-induced cell death might be specific for a very narrow range of cells during neural development.

To confirm the possibility that CD99 might function in a stage-specific manner, it is important to investigate whether this is also the case during development in normal tissues. This possibility is now being tested experimentally in this laboratory.

In summary, CD99 induces apoptosis in ES cell lines through CsA-inhibitable mitochondrial PT pore opening, the reduction of the  $\Delta\Psi_m$ , and caspase activation. By analogy with the role of CD99 in thymocytes, the finding that CD99-induced cell death was confined only in undifferentiated ES cells suggests a specific role of CD99 in the apoptosis during a particular stage of neural development. Therefore, we hypothesize that CD99 might play a certain role in the apoptosis of the undifferentiated form of neural progenitor cells during the development of the nervous system *in vivo*. Furthermore, the result that CD99 induced cell death only in ES cells might open up the possibility that CD99 can be used as an immunotherapeutic tool for ES patients.

### Acknowledgments

We thank Dr. J. K. Shin (Dana-Farber Cancer Institute, Harvard Medical School, Boston, MA) for a generous gift of FK-506. We are grateful to Dr. I. S. Chung, Dr. H.

Son, and Dr. S. B. Lee for helpful discussion and critical reading.

### References

1. Kerr JFR: Shrinkage necrosis: a distinct mode of cellular death. *J Pathol* 1971, 105:13-20
2. Yazdanbakhsh K, Choi JW, Li Y, Lau LF, Choi Y: Cyclosporin A blocks apoptosis by inhibiting the DNA binding activity of the transcriptional factor Nur 77. *Proc Natl Acad Sci USA* 1995, 92:437-441
3. Ferrer I, Olive M, Ribera J, Planas AM: Naturally occurring (programmed) and radiation-induced apoptosis are associated with selective c-Jun expression in the developing rat brain. *Eur J Neurosci* 1996, 8:1286-1298
4. Kroemer G: The proto-oncogene Bcl-2 and its role in regulating apoptosis. *Nature Med* 1997, 3:614-620
5. Hengartner MO: Death cycle and swiss army knives. *Nature* 1998, 391:441-442
6. Petronilli V, Nicolli A, Costantini P, Colonna R, Bernardi P: Regulation of the permeability transition pore, a voltage-dependent mitochondrial channel inhibited by cyclosporin A. *Biochem Biophys Acta* 1994, 1187:255-259
7. Petronilli V, Cola C, Massari S, Colonna R, Bernardi P: Physiological effectors modify voltage sensing by the cyclosporin A-sensitive permeability transition pore of mitochondria. *J Biol Chem* 1993, 268:21939-21945
8. Crompton M, Ellinger H, Costi A: Inhibition by cyclosporin A of a  $Ca^{2+}$ -dependent pore in heart mitochondria activated by inorganic phosphate and oxidative stress. *Biochem J* 1988, 255:357-360
9. Moll R, Lee I, Gould VE, Berndt R, Roessner A, Franke WW: Immunocytochemical analysis of Ewing's tumors. Patterns of expression of intermediate filaments and desmosomal proteins indicate cell type heterogeneity and pluripotential differentiation. *Am J Pathol* 1987, 127:288-304
10. Cavazzana AO, Miser JS, Jefferson J, Triche TJ: Experimental evidence for a neural origin of Ewing's sarcoma of bone. *Am J Pathol* 1987, 127:507-518
11. Hara S, Adachi Y, Kaneko Y, Fujimoto J, Hata J: Evidence for heterogeneous group of neuronal differentiation of Ewing's sarcoma. *Br J Cancer* 1991, 64:1025-1030
12. Tetsuro S, Akihiro U, Jun-ichi H: Neurogenic potential of Ewing's sarcoma cells. *Virchows Arch* 1997, 430:41-46
13. Noguera R, Triche TJ, Navarro S, Tsokos M, Llombart-Bosch A: Dynamic model of differentiation in Ewing's sarcoma cell lines. *Lab Invest* 1992, 62:143-151
14. Kodama K, Doi O, Higashiyama M, Yokouchi H, Tateishi R, Mori Y: Differentiation of a Ewing's sarcoma cell line towards neuronal and mesenchymal cell lineages. *Jpn J Cancer Res* 1994, 85:335-338
15. Gelin CF, Aurit F, Phalipon A, Raynal B, Cole S, Kaczorek M, Bernard A: The E2 antigen, a 32 kD glycoprotein involved in T-cell adhesion process, is the MIC2 gene product. *EMBO J* 1989, 8:3253-3259
16. Dworzak MN, Fritsch G, Buchinger P, Fleischer C, Printz D, Zellner A, Schöllhammer A, Steiner G, Ambros PF, Gadner H: Flow cytometric assessment of human MIC2 expression in bone marrow, thymus, and peripheral blood. *Blood* 1994, 83:415-425
17. Fellingner EJ, Garin-Chesa P, Triche TJ, Huvos AG, Rettig WJ: Immunohistochemical analysis of Ewing's sarcoma cell surface antigen p30/32<sup>MIC2</sup>. *Am J Pathol* 1991, 139:317-325
18. Bernard G, Zoccola D, Deckert M, Breittmayer J-P, Aussel C, Bernard A: The E2 molecule (CD99) specifically triggers homotypic aggregation of CD4<sup>+</sup>CD8<sup>+</sup> thymocytes. *J Immunol* 1995, 154:26-32
19. Hahn J-H, Kim MK, Choi EY, Kim SH, Sohn HW, Ham DI, Chung DH, Kim TJ, Lee WJ, Park CK, Ree HJ, Park SH: CD99 (MIC2) regulates the LFA-1/ICAM-1-mediated adhesion of lymphocytes, and its gene encodes both positive and negative regulators of cellular adhesion. *J Immunol* 1997, 159:2250-2258
20. Choi EY, Park WS, Jung KC, Kim SH, Park SH: Engagement of CD99 induces upregulation of TCR and MHC I and II molecules on the surface of human thymocytes. *J Immunol* 1998, 161:749-754
21. Bernard G, Breittmayer J-P, Matteis M, Trampont P, Hofman P, Senik A, Bernard A: Apoptosis of immature thymocytes mediated by E2/CD99. *J Immunol* 1997, 158:2543-2550



22. Jung KC, Kim TJ, Chung DH, Lee GK, Hahn J-H, Park SH: An antibody against E2/MIC2 antigen (CD99): identification and characterization. *J Kor Cancer Assoc* 1996, 28:350-358
23. Traganos F, Melamed MR, Darzynkiewicz Z: Single step procedure for labeling DNA strand breaks with fluorescein- or BODIPY-conjugated deoxynucleotides: detection of apoptosis and bromodeoxyuridine incorporation. *Cytometry* 1995, 20:172-180
24. Zamzami N, Marchetti P, Castedo M, Zanin C, Vayssière J-L, Petit PX, Kroemer G: Reduction in mitochondrial potential constitutes an early irreversible step of programmed lymphocytes death in vivo. *J Exp Med* 1995, 181:1661-1672
25. Kover H, Dworzak M, Strehl S, Kovar H, Gadner H, Sazler-Kuntschik M: Overexpression of the pseudoautosomal gene MIC2 in Ewing's sarcoma and peripheral primitive neuroectodermal tumor. *Oncogene* 1990, 5:1067-1070
26. Ida K, Kobayashi S, Taki T, Hanada R, Bessho F, Yamamori S, Sugimoto T, Ohki M, Hayashi Y: *EWS-FLI-1* and *EWS-ERG* chimeric mRNA in Ewing's sarcoma and primitive neuroectodermal tumor. *Int J Cancer* 1995, 63:500-504
27. Rettig WJ, Garin-Chesa P, Huvos AG: Ewing's sarcoma: new approaches to histogenesis and molecular plasticity. *Lab Invest* 1992, 66:133-137
28. Zamzami N, Marchetti P, Castedo M, Decaudin D, Macho A, Hirsch T, Susin SA, Petit PX, Mignotte B, Kroemer G: Sequential reduction of mitochondrial transmembrane potential and generation of reactive oxygen species in early programmed cell death. *J Exp Med* 1995, 182:367-377
29. Kroemer G, Petit PX, Zamzami N, Vayssière J-L, Mignotte B: The biochemistry of apoptosis. *FASEB J* 1995, 9:1277-1287
30. Ankarcrona M, Dypbukt JM, Bonfoco E, Zhivotovsky B, Orrenius D, Lipton SA, Nicotera P: Glutamate-induced neuronal death: a succession of necrosis or apoptosis depending on mitochondrial function. *Neuron* 1995, 15:961-973
31. Fruman DA, Klee CB, Bierer BE, Burakoff SJ: Calcineurin phosphatase activity in T lymphocytes is inhibited by FK506 and cyclosporin A. *Proc Natl Acad Sci USA* 1992, 89:3686-3690
32. Petit PX, O'Connor JE, Grunwald D, Brown SC: Analysis of the membrane potential of rat and mouse liver mitochondria by flow cytometry and possible application. *Eur J Biochem* 1990, 389-397
33. Ross T, Olivier R, Monney L, Rager M, Conu S, Fellay I, Jansen B, Borner C: Bcl-2 prolongs cell survival after Bax-induced release of cytochrome c. *Nature* 1998, 391:496-499
34. Martinou J-C, Sadoul R: ICE-like proteases execute the neuronal death program. *Curr Opin Neurobiol* 1996, 6:609-614
35. Sakahira H, Enari M, Nagata S: Cleavage of CAD inhibitor in CAD activation and DNA degradation during apoptosis. *Nature* 1998, 391:96-99